



ISTITUTO NAZIONALE DI RICERCA METROLOGICA Repository Istituzionale

Calibration of multicomponent force and moment transducers using uniaxial force standard machines integrated with tilted plates

This is the author's submitted version of the contribution published as:

Original

Calibration of multicomponent force and moment transducers using uniaxial force standard machines integrated with tilted plates / Prato, A; Borgiattino, D; Facello, A; Mazzoleni, F; Germak, A. - In: MEASUREMENT SCIENCE & TECHNOLOGY. - ISSN 0957-0233. - 33:9(2022), pp. 1-13. [10.1088/1361-6501/ac793c]

Availability:

This version is available at: 11696/74819 since: 2023-06-05T15:27:47Z

Publisher:

IOP Publishing Ltd

Published

DOI:10.1088/1361-6501/ac793c

Terms of use:

This article is made available under terms and conditions as specified in the corresponding bibliographic description in the repository

Publisher copyright

Institute of Physics Publishing Ltd (IOP)

IOP Publishing Ltd is not responsible for any errors or omissions in this version of the manuscript or any version derived from it. The Version of Record is available online at DOI indicated above

(Article begins on next page)

Calibration of multicomponent force and moment transducers using force standard machines integrated with tilted plates

Andrea Prato, Davide Borgiattino, Alessio Facello, Fabrizio Mazzoleni and Alessandro Germak

INRIM – National Institute of Metrological Research, Division of Applied Metrology and Engineering,
Strada delle Cacce 91, 10135 Torino, Italy

E-mail: a.prato@inrim.it

Abstract

Traceability of multicomponent force and moment transducers is a metrological priority as stated within the document of future strategy 2017 to 2027 of the Consultative Committee of Mass and Related Quantities of BIPM. In this paper, a calibration system using force standard machines integrated with tilted plates is described. The main advantage of this method is the possibility to apply forces and moments using existing force standard machines without the necessity to modify them or to develop specific ones. On the other hand, forces and moments cannot be independently applied. Expanded uncertainties of the applied side forces and moments are in the order of around 5 %. A procedure for the calibration and the uncertainty assessment of multicomponent force and moment transducers is also provided. Calibration results, in terms of main and cross-talk sensitivities, of a six-components transducer are shown. This method is easily implementable and can be adopted to improve the current standard.

Keywords: calibration, multi-component, force and moment transducer, sensitivity matrix

1. Introduction

The demand of multicomponent force and moment transducers (MCFMTs) has hugely increased in the last decades. Such devices are typically used in the field of automating industrial plants, through, for example, the use of anthropomorphic robots or robot cells [1-3], in civil and aerospace engineering for wind tunnel balances [4-5], and in quality and production engineering for machine operations and applications [6-7].

Currently, few national metrology institutes have developed specific calibration systems for this kind of transducers. At PTB (Physikalisch Technische Bundesanstalt) a hexapod-structured calibration machine equipped with six servo motors able to generate forces up to 10 kN and moments up to 1 kN·m [8,9] and a deadweight force and torque machine equipped with additional weights able to generate a vertical

force up to 1 MN and a torque up to 2 kN·m [10] have been developed. The first is the only available machine that can generate any combination of forces and moments and is declared with an uncertainty level of 2×10^{-4} . The second is an adaptation of a deadweight machine and is addressed to two-components transducers. In Korea, two multicomponent forces and moments calibration machines have been devised using deadweights and a system of stainless steel wires, ball screws and step motors, generating forces up to 500 N and moments up to 50 N·m [11] and continuous forces up to 2 kN and moments up to 0.4 kN·m [12], at an uncertainty level of few parts in 10^{-4} . At INRiM (Istituto Nazionale di Ricerca Metrologica) deadweight force standard machines (FSMs) have been equipped with a system of pulleys and bell crank levers [13,14] in order to generate vertical forces up to 105 kN, side forces up to 6 kN and moments up to 2 kN·m, at an uncertainty level of 3×10^{-4} . However, this system has the disadvantage of occupying a large area of 50 m² and some

parts of the FSMs have to be rearranged each time before starting the calibration. Another calibration system using two graduated rotating tables with a mass has been developed for forces up to 200 N and moments up to 15 N·m but it is addressed only to particular low-capacity transducers used in robotics [15].

At present, an international traceability chain for multicomponent forces and moments, as well as a defined calibration method for such transducers and testing machines, is still lacking. For this reason, as reported by the BIPM strategy document 2017-2027 by the Consultative Committee for Mass and Related Quantities, «the working group will consider multicomponent force measurement and comparisons under consideration of parasitical components» [16]. The main problems related to the calibration of these transducers are the simultaneous generation of different force and moment components necessary to represent the typical use of these transducers, the costs in developing ad-hoc calibration machines, the large number of tests to get a suitable experimental plan to reach the lowest required uncertainty level and the lack of suitable calibration and uncertainty assessment procedures.

In this paper, a calibration system for multicomponent force and moment transducers based on the use of existing FSMs integrated with tilted plates is investigated to find a compromise to all these issues. A proper calibration procedure, which allows to simultaneously evaluate the main and cross-talk sensitivities of the six force and moment components, is also proposed. A preliminary version of the method was previously investigated for the characterization of a high capacity MCFMT, however without any evaluation of the efficacy of the experimental plan and any assessment of the uncertainty budget [17].

The calibration system with the uncertainty assessment of the applied reference force or moment components is presented in Section 2. The calibration method and procedure, together with two uncertainty assessment methods according to GUM [18] in matrix form and in analogy to ISO 376 [19], are described in Section 3. Calibration measurements are then performed and applied to a MCFMT with a vertical force capacity of 100 kN. The main sensitivities and the related cross-talk terms with the associated uncertainties are determined and shown in Section 4.

2. FSMs integrated with tilted plates

2.1 The equations of the reference forces and moments

The system adopted for the generation of the different force and moment components involves the use of existing FSMs integrated with a couple of hardened steel tilted plates, between which the MCFMT under calibration is placed as depicted in figure 1. Modulating the angle of tilt, rotating the transducer around its axis and misaligning it with respect to

the machine loading axis, it is possible to decompose the reference force F generated by the FSM with the result of generating vertical and side forces and bending and torsion moments. The relevant equation can be easily obtained from elementary trigonometrical laws. Naming xyz and $x'y'z'$ the tilted plates and the transducer reference systems, respectively, both centred at the centre of the transducer and considering a tilt angle α of the plates, a MCFMT of height h , an anticlockwise (from the top) rotation angle ω , d_x and d_y misalignments along x - and y -axis, respectively, it is possible to get the equations of the six reference forces and moments generated with the tilted plates and acting on the MCFMT under calibration, according to equation 1 and figures 2 and 3.

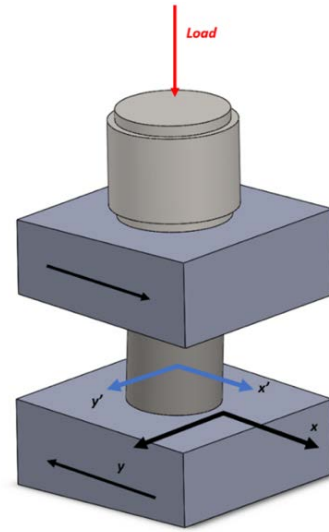


Figure 1. Scheme of a MCFMT between the 2° tilted plates under the load of the FSM.

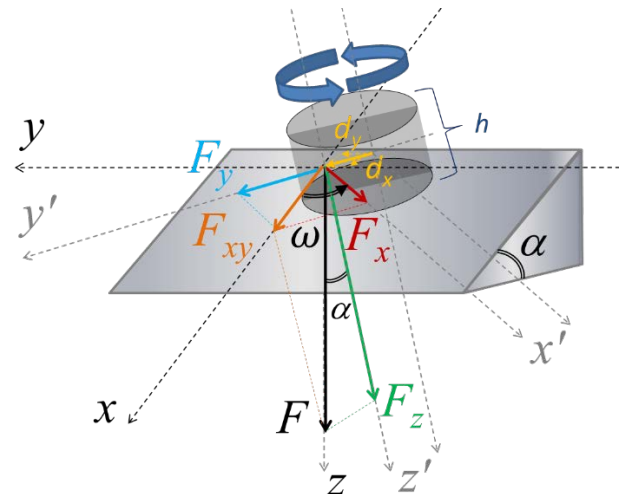


Figure 2. 3-D scheme of the forces and moments generated with the tilted plates on the MCFMT.

$$\left\{ \begin{array}{l} F_x = F \cdot \sin \alpha \cdot \cos \omega \\ F_y = F \cdot \sin \alpha \cdot \sin \omega \\ F_z = F \cdot \cos \alpha \\ M_x = F \cdot \cos \alpha \cdot \sqrt{d_x^2 + d_y^2} \cdot \sin(i\omega + j\theta) + \frac{F \cdot \sin \alpha \cdot \sin \omega \cdot h}{2} \\ M_y = -iF \cdot \cos \alpha \cdot \sqrt{d_x^2 + d_y^2} \cdot \cos(k\omega + \theta) - \frac{F \cdot \sin \alpha \cdot \cos \omega \cdot h}{2} \\ M_z = F \cdot \sin \alpha \cdot d_y \end{array} \right. \quad (1)$$

Where $\theta = \left| \tan^{-1} \left(\frac{d_y}{d_x} \right) \right|$ and $i=+1, j=+1, k=+1$ for $d_x > 0$ and $d_y > 0$; $i=-1, j=+1, k=-1$ for $d_x < 0$ and $d_y > 0$; $i=+1, j=-1, k=-1$ for $d_x > 0$ and $d_y < 0$; $i=-1, j=-1, k=+1$ for $d_x < 0$ and $d_y < 0$.

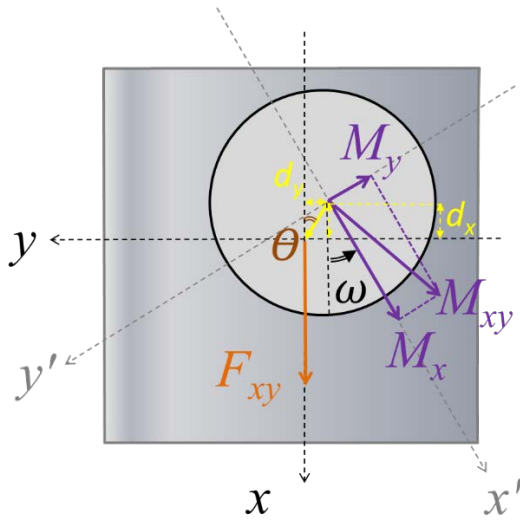


Figure 3. Top view scheme of the side forces and bending moments generated with the tilted plates on the MCFMT

2.2 Reference forces and moments and uncertainty assessment

In the previous Section, it is shown that applied forces and moments depend on the geometrical boundary conditions. From equation (1), generated side forces and moments increase at increasing height of the transducer, tilt angles, and misalignments. However, geometrical boundary conditions have to be cautiously chosen in order to guarantee the stability of the whole structure during load, which, in turn, depends on the friction between the tilted plates and transducer surfaces. For this reason, four couples of hardened steel (34CrNiMo6) tilted plates with angles of 0°, 1°, 2° and 3° are designed and manufactured to be installed in the deadweight FSMs at INRiM. Each plate is 200×200×70 mm³ and weighs around 30 kg. The dimensions and tilt angles of the plates are cautiously chosen in order to fit the load platform of the machines and to guarantee the stability of the system under high loads, considering steel-to-steel friction between the

tilted plate and a typical transducer. An example representing the 1 MN deadweight FSM integrated with tilted plates is shown in figure 4. A double-knife joint is interposed between the loading frame of the machine and the upper plate in order to avoid the generation of spurious components.



Figure 4. The 1 MN deadweight FSM integrated with 3° tilted plates at INRiM.

By way of example, in the 100 kN deadweight FSM integrated with the above-mentioned four couples of tilted plates, considering a transducer height of 77 mm and misalignments d_x and d_y along x- and y-axis up to 16 mm, the maximum applied forces and moments can be calculated according to equation (1) and summarized in table 1.

These values cannot be independently generated since each component depends on the chosen boundary condition. For example, the highest positive force along x-axis, $F_x=5233.6$ N, is obtained with $F=100$ kN, $\alpha=3^\circ$ and $\omega=0^\circ$, while the highest positive bending moment along y-axis, $M_y=2402.1$ N·m, is obtained with $F=100$ kN, $\alpha=3^\circ$, $\omega=135^\circ$,

$d_x=16$ mm and $d_y=16$ mm. To increase these values, larger tilt angles and misalignments are needed, compatibly with the stability of the structure. This could be obtained by increasing the friction between the tilted plate/transducer contact surface.

Table 1. Maximum positive or negative applied forces and moments with the associated relative expanded uncertainty in the 100 kN deadweight FSM with the above-mentioned boundary conditions.

Component	Max. Value	Rel. exp. unc.
F_x	5233.6 N	3.8×10^{-2}
F_y	5233.6 N	3.8×10^{-2}
F_z	100 kN	2.0×10^{-5}
M_x	2402.1 N·m	4.8×10^{-2}
M_y	2402.1 N·m	4.8×10^{-2}
M_z	83.7 N·m	8.2×10^{-2}

Uncertainties associated with the highest applied reference forces (F_x , F_y , F_z) and moments (M_x , M_y , M_z) are evaluated according to GUM [18] by propagating the individual uncertainty contributions of the input parameters, shown in equation (1): the reference force F generated by the FSM, the tilt angle α , the rotation angle ω , the MCFMT height h , and the d_x and d_y misalignments along x - and y -axis, respectively. Standard uncertainty $u(F)$ associated with the reference force F generated by the FSM derives from the Calibration and Measurement Capabilities (CMC) declared by INRiM [25], which is 2×10^{-6} in terms of relative expanded uncertainty. Standard uncertainties associated with the tilted plate angle $u(\alpha)$ and to the rotation angle $u(\omega)$ are considered as type B uncertainty contributions with half-widths of 0.1° and 2° , respectively, and uniform rectangular distribution. These values are given by the fact that tilted plates are realised with numerical control machines (tolerance of $\pm 0.1^\circ$), whereas the rotation of the MEMS is manually performed following the centring lines drawn on the tilted plates. Standard uncertainties associated with the MCFMT height $u(h)$ and to the misalignments $u(d_x)$ and $u(d_y)$ are considered as type B uncertainty contributions with half-widths of ± 1 mm. This is a cautious esteem of the random errors occurring during the alignment of the MCFMT and the tilted plates with respect to the axis of the machine. Alignments are rigorously performed before each measurement by means of levellers, callipers and reference blocks, as described below in Section 3.2. As expected, uncertainty associated with the vertical force F_z is much lower than the other components which, on average, are between 4 % and 8 %. This is due to the higher number of input parameters involved.

By way of example, the detailed uncertainty budget for the highest reference bending moment $M_y=2402.1$ N·m is shown in table 2. It is obtained that the relative expanded uncertainty (at a confidence level of 95 %, i.e. coverage factor equal to 2)

is 4.8 %. The major individual contributions to the combined standard uncertainty are due to the misalignments d_x and d_y . The third uncertainty contribution is due to the rotation angle ω , while the fourth and fifth uncertainty contributions are due to the angle of tilt α and to the MCFMT height h . Uncertainty contribution due to the reference force F generated by the FSM is negligible compared to the other terms. Similar behaviour is found for the other components.

Table 2. Uncertainty table (according to GUM) for the reference bending moment M_y .

Variable x_k		$u^2(x_k)$	c_k	$u_k^2(M_y)$	Rank
Symbol	Value				
F	100 kN	1.0E+00	2.4E-02	5.8E-04	6
α	3°	3.3E-03	4.5E+01	6.9E+00	4
ω	135°	1.3E+00	2.5E+00	8.2E+00	3
d_x	0.016 m	3.3E-07	7.1E+04	1.7E+03	1
d_y	0.016 m	3.3E-07	7.1E+04	1.7E+03	2
h	0.100 m	3.3E-07	3.7E+03	4.6E+00	5
M_y	2402.1 N·m	Std. uncert. $u(M_x)$		57.8 N·m	
		Exp. uncert. $U(M_x)$		115.7 N·m	

3. Calibration procedure and uncertainty assessment of a MCFMT

Similarly to uniaxial force transducers, most of MCFMTs are composed of different strain-gauge bridges, each dedicated to a specific component to be measured. The intrinsic influence between the different components, however, cannot be ignored, and cross-talk signals for combined axial forces and moments must be examined in calibration operations [20]. Therefore, calibration measurements with various combinations of applied forces and moments are essential for accurately evaluating sensitivity or exploitation matrix terms. According to Ronald Fisher's seminal work from 1926 [21], the calibration experimental plan has a huge impact on the measured sensitivities and related uncertainties. A calibration experimental plan composed of a set of applied forces and moments with high correlations between these components results in a poorly conditioned matrix, which, when inverted, produces poorly defined outcomes with increased uncertainty. As a result, in calibration operations, a suitable experimental strategy connected to the needed level of accuracy and uncertainty must be established. If the lowest level of uncertainty is desired, a full factorial experimental plan with a large number of applied loads should be used, resulting in longer times and higher costs. If higher uncertainties are tolerable, however, fewer measurements can be carried out. This premise is necessary to understand the development of the calibration procedure here proposed. Such procedure is applied to a MCFMT (*HBM MCS10-100-6C*) with nominal capacities of $F_{x,c}=F_{y,c}=20$ kN, $F_{z,c}=100$ kN, $M_{x,c}=M_{y,c}=2000$ N·m and

$M_{z,c}=1500 \text{ N}\cdot\text{m}$. The MCFMT, shown in figure 5, has six independent outputs each one dedicated to a single component. The height and diameter are 77 mm and 86 mm, respectively. The transducer is connected to an HBM MGCPlus amplifier (resolution of 0.00001 mV/V). Measurements are performed in the INRiM 1 MN deadweight FSM (instead of the 100 kN machine in order to guarantee faster operation) integrated with tilted plates previously described and shown in figure 4. An experimental plan with $n=520$ calibration conditions is applied. The main sensitivities and the related cross-talk terms are determined in matrix form, as well as the exploitation matrix, whose terms are the ones used by end-users. The detailed uncertainty budget is evaluated according to GUM [18] in two ways: in matrix form and in analogy to ISO 376 [19].



Figure 5. The MCFMT under test.

3.1 The calibration experimental plan

As previously stated, it is of fundamental importance to use an experimental plan capable of covering all possible combinations of forces and moments in order to obtain matrices not subjected to poor conditioning. Avoiding correlations between variables is also important to satisfy some assumptions behind the calculation and propagation of uncertainty. Since a full factorial experimental plan is not applicable with this calibration system since each component cannot be independently applied, the starting point is the definition of the values for each independent parameter in order to have, at the same time, a feasible number of measurements to be performed and a wide number of combinations to minimize the correlation between the applied components [22]. The idea of the proposed experimental plan is to locate the transducer into 4 positions, given by different

d_x and d_y misalignment combinations ($d_x=0 \text{ mm } d_y=0 \text{ mm}$; $d_x=8 \text{ mm } d_y=0 \text{ mm}$; $d_x=0 \text{ mm } d_y=16 \text{ mm}$; $d_x=16 \text{ mm } d_y=8 \text{ mm}$) and at 4 different tilt angles α ($0^\circ, 1^\circ, 2^\circ$ and 3°) and 7 rotations ω ($0^\circ, 45^\circ, 90^\circ, 135^\circ, 180^\circ, 270^\circ, 360^\circ$), and to apply 4 different load levels F (10 %, 50 %, 80 % and 100 % of the maximum applied force). The number of these measurements is 448 (4 positions \times 4 tilt angles \times 7 rotations \times 4 loads). These misalignments and tilt angles are cautiously chosen in order to guarantee the stability of the whole system and to avoid any overloads of the MCFMT outputs. To these combinations, 72 more calibration conditions including negative misalignments (up to $d_x=-16 \text{ mm}$ and $d_y=-16 \text{ mm}$) are added in order to apply positive torsion moments and to evaluate the uncertainty in analogy to ISO 376 also for this component (see Section 3.5). Therefore, a total of 520 measurements are performed. Maximum applied loads (positive or negative) for each component are summarized in table 3. If on one hand, applied reference vertical force and bending moments are applied up to around 100 % of the maximum capacity of the MCFMT, on the other hand, side forces and torque are much lower. However, at this stage of the research, mainly focused on the method rather than on the magnitude of the applied forces and moments, this condition is accepted in order to avoid possible problems of stability and safety of the structure. Extensions of these parameters will be evaluated in the future through appropriate simulations and experimental measurements.

The whole experimental plan for each couple of components is shown in figure 6. Correlation values between each couple of generated forces and moments range from -0.37 to 0.32, thus should guarantee minimized uncertainty levels. It is also worth noting that, since a high but unavoidable number of combinations have side forces and torsion moments close to zero, the uncertainties associated with their cross-talk effects are expected to be higher compared to the others, as detailed in Section 4.2.

Table 3. Maximum positive or negative applied reference forces and moments.

	<i>Max. applied component</i>	<i>Max. values / MCFMT capacity ratio</i>
F_x	5233.6 N	26 %
F_y	5233.6 N	26 %
F_z	100000 N	100 %
M_x	1837.2 N·m	92 %
M_y	1837.2 N·m	92 %
M_z	83.7 N·m	6 %

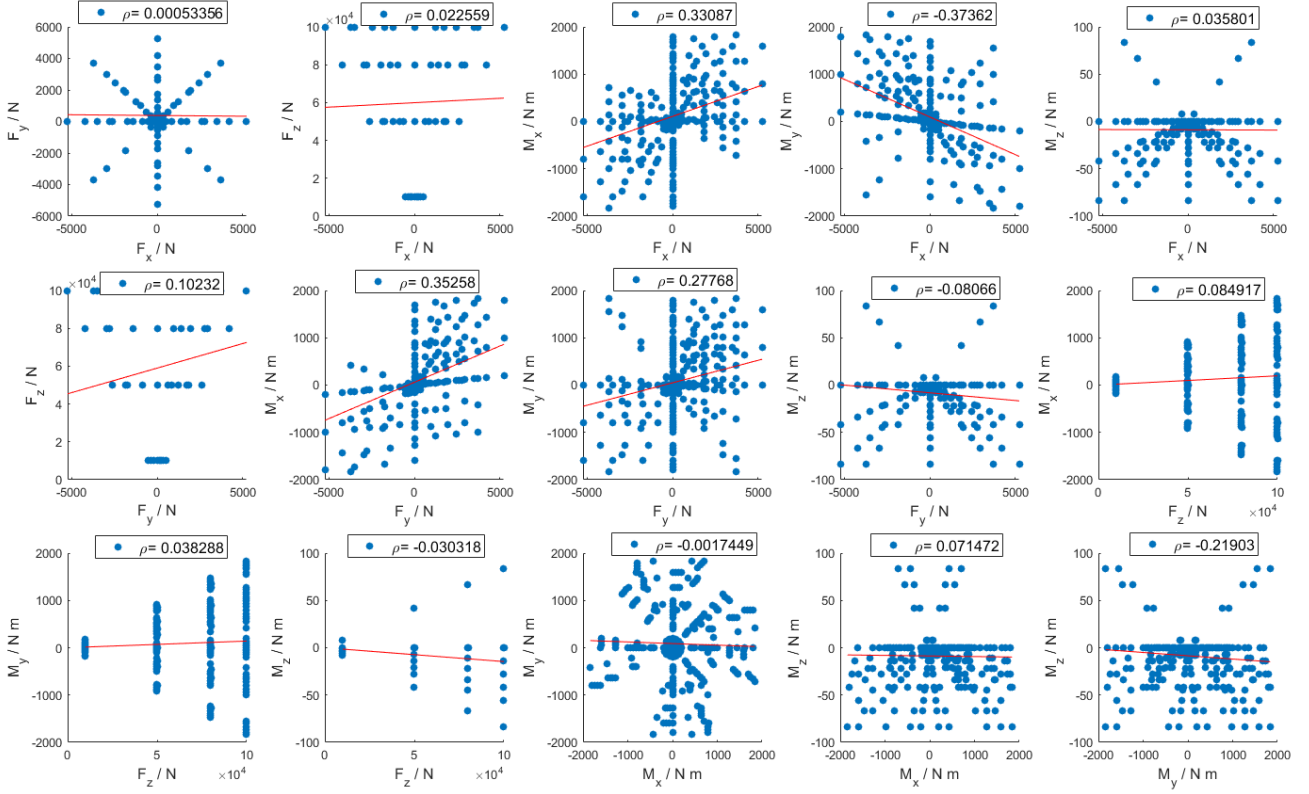


Figure 6. The calibration experimental plan with the 520 measurement conditions for each couple of components.

3.2 Alignment procedure and data acquisition

Alignment of the tilted plates and the MCFT is one of the crucial aspects to get accurate results. This operation includes the centring of the frame in relation to the joint, the centring of the joint in relation to the plate, the control of the correct position and orientation of the transducer and the tilted plates. Such procedure is performed by means of soft head rubber mallets to move the plates or for large displacements of the transducer, an aluminium rod used like a chisel to make more precise shifts (moving the transducer directly with the hammer would make it difficult to follow a straight path because of the difficulty of striking in the same point), a calliper set to length for centring the transducer and for centring the double-knife joint relative to the machine frame, calibrated blocks for centring operations and another hammer for small shifts and finishing touches. For this reason, a type B uncertainty contribution of ± 1 mm is assigned to misalignments, as shown in Section 2.2.

MCFMT outputs are acquired by the 6-channels amplifier powered at 10 V and 600 Hz. The output signals are filtered with a Bessel filter at 0.05 Hz. To optimize the calibration process, the transducer is firstly placed in the correct position and the indicator is zeroed, then increasing loads are applied. Data are acquired 30 s after the application of each load. The return-to-zero acquisition is performed after the application of the maximum load.

3.3 Evaluation of the exploitation and sensitivity matrices

Every output of an ideal MCFMT is only dependent on the relevant force or moment component. Actually, this is not true because transducer outputs interact with one another, and cross-talk sensitivities may be important. In first analysis, each force and moment component F_k ($k=1, 6$) can be expressed as a linear combination of the MCFMT outputs d_i ($i=1, 6$) with second-order interactions ignored, as shown in equation (2) e equation (3) in general matrix form.

$$\begin{cases} F_x = d_1 A_{11} + d_2 A_{21} + d_3 A_{31} + d_4 A_{41} + d_5 A_{51} + d_6 A_{61} \\ F_y = d_1 A_{12} + d_2 A_{22} + d_3 A_{32} + d_4 A_{42} + d_5 A_{52} + d_6 A_{62} \\ F_z = d_1 A_{13} + d_2 A_{23} + d_3 A_{33} + d_4 A_{43} + d_5 A_{53} + d_6 A_{63} \\ M_x = d_1 A_{14} + d_2 A_{24} + d_3 A_{34} + d_4 A_{44} + d_5 A_{54} + d_6 A_{64} \\ M_y = d_1 A_{15} + d_2 A_{25} + d_3 A_{35} + d_4 A_{45} + d_5 A_{55} + d_6 A_{65} \\ M_z = d_1 A_{16} + d_2 A_{26} + d_3 A_{36} + d_4 A_{46} + d_5 A_{56} + d_6 A_{66} \end{cases} \quad (2)$$

$$\mathbf{F} = \mathbf{d} \mathbf{A} \quad (3)$$

where \mathbf{F} is the row $1 \times k$ reference forces and moments matrix, \mathbf{d} is the $1 \times i$ matrix of the MCFMT outputs, and \mathbf{A} is the $i \times k$ coefficients matrix, also called exploitation matrix, which is the matrix actually used by end-users. In this specific case, matrix \mathbf{A} is a 6×6 squared matrix. $A_{i,k}$ are the coefficients of

the the MCFMT outputs d_i used to calculate the force and moment components F_k .

Considering the $n=520$ linearly independent sets of calibration values deriving from the experimental plan, \mathbf{F} and \mathbf{d} , in equation (3), become a $n \times k$ and a $n \times i$ matrix, respectively. From simple calculation applied to equation (3), matrix \mathbf{A} and its $A_{i,k}$ coefficients can be evaluated according to equation (4) [23].

$$\mathbf{A} = [\mathbf{d}^T \mathbf{d}]^{-1} \mathbf{d}^T \mathbf{F} \quad (4)$$

In the same way, to evaluate sensitivity matrix, considering $n=520$ linearly independent sets of values, each MCFMT output d_i ($i=1, 6$) can be expressed as a linear combination of the force and moment components F_k ($k=1, 6$), according to equation (5),

$$\mathbf{d} = \mathbf{F} \mathbf{A}^{-1} = \mathbf{F} \mathbf{S} \quad (5)$$

where \mathbf{S} is the $k \times i$ (6×6) sensitivity matrix, in which the diagonal terms are the main sensitivities, and the out-of-diagonal terms are the cross-talk sensitivities. The sensitivity matrix is the inverse of the exploitation matrix, $\mathbf{S} = \mathbf{A}^{-1}$, if $i=k$.

3.4 Uncertainty assessment in matrix form

A comprehensive uncertainty evaluation of A_{ij} terms can be performed according to GUM [18,22]. The $i \times k$ (6×6) matrix of the variances referred to the single terms of the exploitation matrix, $\mathbf{u}^2(\mathbf{A})$, is given by the general rule of uncertainty propagation, according to equation (6),

$$\begin{aligned} \mathbf{u}^2(\mathbf{A}) &= \begin{bmatrix} u^2(A_{11}) & \cdots & u^2(A_{1k}) \\ \vdots & \ddots & \vdots \\ u^2(A_{i1}) & \cdots & u^2(A_{ik}) \end{bmatrix} = \\ &= \begin{bmatrix} u^2(A_{11})' & \cdots & u^2(A_{1k})' \\ \vdots & \ddots & \vdots \\ u^2(A_{i1})' & \cdots & u^2(A_{ik})' \end{bmatrix} \\ &+ \begin{bmatrix} u^2(S_{11}) \frac{A_{11}^2}{S_{11}^2} & \cdots & u^2(S_{1i}) \frac{A_{11}^2}{S_{1i}^2} \\ \vdots & \ddots & \vdots \\ u^2(S_{k1}) \frac{A_{1k}^2}{S_{k1}^2} & \cdots & u^2(S_{ki}) \frac{A_{ik}^2}{S_{ki}^2} \end{bmatrix}^T \end{aligned} \quad (6)$$

where,

$$\begin{bmatrix} u^2(A_{11})' & \cdots & u^2(A_{1k})' \\ \vdots & \ddots & \vdots \\ u^2(A_{i1})' & \cdots & u^2(A_{ik})' \end{bmatrix} = \mathbf{c} \mathbf{u}^2(\mathbf{F}) \quad (7)$$

is the $i \times k$ (6×6) matrix given by multiplying \mathbf{c} , which is a $i \times n$ (6×520) matrix of the squared terms of $[\mathbf{d}^T \mathbf{d}]^{-1} \mathbf{d}^T$ matrix, and $\mathbf{u}^2(\mathbf{F})$, which is the $n \times k$ (520×6) matrix representing the variances of the reference applied forces and moments at each calibration condition, as described in Section 2.2. $u^2(S_{ki})$ are the terms deriving from,

$$\begin{bmatrix} u^2(S_{11}) & \cdots & u^2(S_{1i}) \\ \vdots & \ddots & \vdots \\ u^2(S_{k1}) & \cdots & u^2(S_{ki}) \end{bmatrix} = \mathbf{h} \mathbf{u}^2(\mathbf{d}) \quad (8)$$

which is the $k \times i$ (6×6) matrix given by multiplying \mathbf{h} , a $k \times n$ (6×520) matrix composed of the squared terms of $[\mathbf{F}^T \mathbf{F}]^{-1} \mathbf{F}^T$ matrix, and $\mathbf{u}^2(\mathbf{d})$, which is the $n \times i$ (520×6) matrix representing the variances of the MCFMT outputs containing, for each component, type B uncertainty contributions due to repeatability at rotations 0° and 360° , $u_{\text{rep}}^2(d_i)$, zero drift, $u_{\text{f0}}^2(d_i)$, and resolution of the indicator, $u_{\text{res}}^2(d_i)$. These contributions are combined, for each force and moment component, according to:

$$u^2(d_i) = u_{\text{re}}^2(d_i) + u_{\text{f0}}^2(d_i) + u_{\text{res}}^2(d_i) \quad (9)$$

where $u_{\text{re}}(d_i)$ is the maximum difference between the MCFMT outputs at rotations of 0° and 360° divided by $\sqrt{3}$, in analogy with ISO 376, $u_{\text{f0}}(d_i)$ is the maximum zero error, and $u_{\text{res}}(d_i)$ is the resolution of the MCFMT output divided by $\sqrt{3}$, similarly to ISO 376. Unlike ISO 376, the contributions due to reproducibility and reversibility cannot be evaluated since cross-talk terms are unknown a priori and loads and unloads for a single component of the of MCFMTs cannot be implemented in the calibration experimental plan. The contribution due to the interpolation error is included in the matrix operations.

These operations with matrices and the assumption that $u^2(A_{ik}) = u^2(A_{ik})' + u^2(S_{ki}) A_{ik}^2 / S_{ki}^2$, are due to the impossibility to directly propagate $[\mathbf{d}^T \mathbf{d}]^{-1} \mathbf{d}^T$ matrix terms of equation (4). Expanded uncertainties matrix (at a confidence level of 95% with $k=2$) associated to the exploitation matrix, $\mathbf{U}(\mathbf{A})$, is calculated from the matrices of the variances, $\mathbf{u}^2(\mathbf{A})$, by applying the classical formula to every element of the matrix, i.e. $U(A_{ik}) = 2\sqrt{u^2(A_{ik})}$.

3.5 Uncertainty assessment in analogy to ISO 376

Uncertainties described in the previous Section do not directly refer to the force and moment values but to the exploitation or sensitivity matrix terms. To get an uncertainty directly related to the measured forces and moments, in analogy to ISO 376 for uniaxial force transducers, the matrix \mathbf{A} can be seen as the analogue of the interpolating polynomial in uniaxial force transducer calibrations, the link between the transducer output values (in mV/V) and the force and moment values (in N or N·m). Hence, multiplying the transducer output data d_i by the exploitation matrix \mathbf{A} , forces and moments F_l ($l=k=1, 6$) are obtained. These can be treated separately for the calculation of the uncertainty, as if they were six independent transducers, thus taking also into account the cross-talk terms. In this way, it is possible to calculate the uncertainty, one component at a time, similarly to the prescriptions of ISO 376 [19]. From the 520 tests, 8 load levels ($j=1 \dots 8$), 4 positive and

4 negative for each component (except for F_z for which only compression forces are applied), repeated 3 times ($m=1\dots3$), in different conditions, are found. In this way, the combined standard uncertainty of the l^{th} component at a particular j^{th} load level $u_c(F_{l,j})$ can be calculated as

$$u_c(F_{l,j}) = \sqrt{u_1^2(F_{l,j}) + u_2^2(F_{l,j}) + u_3^2(F_{l,j}) + u_4^2(F_{l,j}) + \Delta(F_{l,j})} \quad (10)$$

where $u_1^2(F_{l,j})$ is the variance associated with the applied calibration force or moment, $u_2^2(F_{l,j})$ is the variance associated with the reproducibility of the calibration results, $u_3^2(F_{l,j})$ is the variance associated with the drift in zero output, $u_4^2(F_{l,j})$ is the variance associated with the resolution of the indicator, and $\Delta(F_{l,j})$ is the mean deviation from the reference load. This last term can be seen as a systematic error and is treated according to the GUM [18] (note to 6.3.1).

Since for a particular l^{th} component, the j^{th} load is obtained with $m=3$ repetitions from three different combinations of the input parameters, uncertainty associated with the applied calibration force $u_1^2(F_{l,j})$ is calculated as the highest $u_1^2(F_{l,j,m})$, among the three repetitions, evaluated as in Section 2.2.

For reproducibility, ISO 376 prescribes three tests, at 0° , 120° and 240° , for different load levels and is expressed as the standard deviation of these measurements. In the case of MCFMTs, reproducibility shall be investigated one component at a time and can be seen as the ability of the transducer to provide the same results, for that specific component, in three repeated tests, following different load combinations of the other components. Therefore, $u_2^2(F_{l,j})$ is evaluated, in analogy to ISO 376, as

$$u_2^2(F_{l,j}) = \frac{\sum_{m=1}^3 (F_{l,j,m} - \overline{F_{l,j}})^2}{6} \quad (11)$$

where $\overline{F_{l,j}}$ is the mean value from the three ($m=1\dots3$) repeated measurements in the different conditions $F_{l,j,m}$.

The variance associated with the drift in zero output $u_3^2(F_{l,j})$ is the maximum zero error (converted in N or N·m) obtained from the calibration measurements (similarly to $u_{f0}(d_i)$, seen in the previous Section), and the variance associated with the resolution of the indicator $u_4^2(F_{l,j})$ is the square of the resolution of the indicator (converted in N or N·m) divided by 12. $\Delta(F_i)$ is calculated as the mean deviation of the three repetitions $F_{l,j,m}$ from the reference applied load $F_{k,j}$:

$$\Delta(F_{l,j}) = \frac{\sum_{m=1}^3 (F_{l,j,m} - F_{k,j})}{3} \quad (12)$$

Iterating this process for all components and all levels, the combined standard uncertainty $u_c(F_{l,j})$ and the expanded uncertainty (at a confidence level of 95 % with a coverage factor equal to 2) $U(F_{l,j})=2u_c(F_{l,j})$, associated with the l^{th} force

and moment component for each j^{th} level, are found. In this way, for each force or moment component, the expanded uncertainties $U(F_{l,j})$ associated with positive-only, negative-only, or both, data are interpolated with a second-order polynomial function as a function of the applied load F_l . In this way, an expanded uncertainty function associated with each component $U(F_l)$ and used by end-users for subsequent operative measurements is found according to:

$$U(F_l) = aF_l^2 + bF_l + c \quad (13)$$

4. Calibration results

4.1 Exploitation and sensitivity matrices

For the evaluation of the exploitation matrix A of the MCFMT under test, 520 measurements are performed, as described in Section 3.1. Each measurement represents a set of the six applied reference forces and moments (F_x , F_y , F_z , M_x , M_y , M_z) and MCFMT outputs (d_1 , d_2 , d_3 , d_4 , d_5 , d_6). Combining all the experimental measurements, the reference forces and moments matrix F and the MCFMT matrix d , both with a dimension of 520×6 , are obtained. In this way, using equations (1)-(4), exploitation matrix A , in N/(mV/V) from column 1 to 3, or in N·m/(mV/V) from column 4 to 6, with the expanded uncertainties (at a confidence level of 95%), are evaluated. Results are reported in equation (14).

$$A = \begin{bmatrix} 14971.5 & -44.4 & 30.6 & 110.0 & -463.3 & 0.6 \\ -13.5 & 14922.0 & -255.6 & 376.2 & 192.8 & -1.5 \\ 2.9 & 106.7 & 80476.4 & 16.3 & 32.7 & -14.0 \\ -11.2 & -16.5 & 177.0 & 1101.1 & -10.0 & -1.7 \\ 31.3 & 51.7 & -245.0 & -10.2 & 1065.4 & 1.8 \\ 1.4 & -38.4 & 1756.8 & -168.7 & -213.5 & 1330.8 \end{bmatrix} \quad (14)$$

Diagonal terms are the main ones since each MCFMT output is nominally sensitive to a particular component. Out-of-diagonal terms range between 0.02 % and 43.49 %, (mean value of around 5 %) of the relevant diagonal term. This is even more visible if the exploitation matrix is normalized by dividing the absolute value of each column term by its associated diagonal component. In this way, normalized exploitation matrix, A^* , is obtained, as shown in equation (15).

$$A^* = \begin{bmatrix} 1.00 & 0.00 & 0.00 & 0.10 & 0.43 & 0.00 \\ 0.00 & 1.00 & 0.00 & 0.34 & 0.18 & 0.00 \\ 0.00 & 0.01 & 1.00 & 0.01 & 0.03 & 0.01 \\ 0.00 & 0.00 & 0.00 & 1.00 & 0.01 & 0.00 \\ 0.00 & 0.00 & 0.00 & 0.01 & 1.00 & 0.00 \\ 0.00 & 0.00 & 0.02 & 0.15 & 0.20 & 1.00 \end{bmatrix} \quad (15)$$

Out-of-diagonal terms are very low except for A_{14} , A_{24} , A_{15} , A_{25} , A_{64} and A_{65} terms, which are related to the sensitivity of d_1 , d_2 and d_6 outputs to M_x and M_y components. Such behaviour was also observed in other strain-gauged MCFMTs [10,17] and is due to the interaction of the relevant Wheatstone bridges of the MCFMTs with the other components.

4.2 Calibration uncertainties in matrix form

Uncertainty assessment in matrix form is carried out according to Section 3.4. The uncertainty matrix $u^2(F)$ of the variances of the reference applied forces and moments at each calibration condition is evaluated according to Sections 2.2. Uncertainty matrix representing the variances of the MCFMT outputs $u^2(d)$, described in Section 3.4, derives from the uncertainty contributions due to reproducibility at rotations of 0° and 360° $u_{\text{rep}}(d_i)$, zero drift $u_{f0}(d_i)$, and resolution of the indicator $u_{\text{res}}(d_i)$, for each component, summarized in table 4. It is worth noting that reproducibility is the major uncertainty contribution, whereas resolution is negligible.

Table 4. Uncertainty contributions associated with the reproducibility $u_{\text{rep}}(d_i)$, zero error $u_{f0}(d_i)$ and resolution $u_{\text{res}}(d_i)$ of the MCFM outputs d_i .

	$u_{\text{rep}}(d_i) / \text{mV/V}$	$u_{f0}(d_i) / \text{mV/V}$	$u_{\text{res}}(d_i) / \text{mV/V}$
F_x	7.13×10^{-3}	1.26×10^{-3}	2.89×10^{-6}
F_y	7.32×10^{-3}	2.74×10^{-3}	2.89×10^{-6}
F_z	7.04×10^{-3}	3.60×10^{-4}	2.89×10^{-6}
M_x	8.09×10^{-2}	7.68×10^{-3}	2.89×10^{-6}
M_y	8.48×10^{-2}	3.66×10^{-3}	2.89×10^{-6}
M_z	6.18×10^{-3}	1.13×10^{-3}	2.89×10^{-6}

In this way, the expanded uncertainty matrix $U(A)$ of the exploitation matrix can be calculated according to equations (6)-(9). Results are shown in equation (16). Relative expanded uncertainties associated with the diagonal terms range between 0.01 % ($U(A_{33})$ related to F_z) and 4.09 % ($U(A_{66})$ related to M_z). In general terms, uncertainties associated with the side forces and bending and torsion moments are higher mainly due to higher uncertainties associated with the applied relevant reference components as shown in Section 2.2.

$$U(A) = \begin{bmatrix} 127.0 & 186.6 & 355.1 & 102.4 & 117.9 & 3.0 \\ 107.5 & 133.0 & 447.1 & 101.8 & 137.9 & 11.4 \\ 21.7 & 16.8 & 71.7 & 16.5 & 12.9 & 1.1 \\ 23.7 & 23.9 & 102.0 & 19.2 & 17.9 & 1.5 \\ 22.8 & 25.8 & 116.3 & 18.9 & 19.0 & 1.3 \\ 525.5 & 557.3 & 2059.6 & 674.4 & 987.3 & 54.5 \end{bmatrix} \quad (16)$$

Out-of-diagonal uncertainties reflect the behaviour of the MCFMT under test and the chosen experimental plan. In particular, it is found that uncertainties associated with the first, second and sixth rows, which represent the cross-talks related to the side forces and the torsion moment, respectively, are higher compared to the others. This is due to the fact that, in a higher number of combinations, side forces and torsion moments are very low, as described in Section 3.1.

4.3 Calibration uncertainties in analogy to ISO 376

Uncertainties are also evaluated according to Section 3.5 in analogy to ISO 376, by converting MCFMT output values in mV/V into N or N·m using the exploitation matrix A

previously found (Section 4.1). With this experimental plan, for each component, 8 load levels (4 positive and 4 negative), except for F_z where only 4 positive load levels can be applied, repeated three times with different combinations, are found. These values are summarized in table 5.

Table 5. The 8 load levels j for each component used for the uncertainty assessment in analogy to ISO 376.

j	F_x / N	F_y / N	F_z / N	$M_x / \text{N}\cdot\text{m}$	$M_y / \text{N}\cdot\text{m}$	$M_z / \text{N}\cdot\text{m}$
1	-5233.6	-5233.6	/	-1600.0	-1600.0	-83.7
2	-4186.9	-4186.9	/	-1280.0	-1280.0	-67.0
3	-2616.8	-2616.8	/	-800.0	-800.0	-41.9
4	-523.4	-523.4	/	-160.0	-160.0	-8.4
5	523.4	523.4	9986	160.0	160.0	8.4
6	2616.8	2616.8	49931	800.0	800.0	41.9
7	4186.9	4186.9	79890	1280.0	1280.0	67.0
8	5233.6	5233.6	99863	1600.0	1600.0	83.7

In this way, uncertainties associated with the applied calibration force or moment, reproducibility, drift in zero output, resolution and the mean deviation from the reference load are evaluated according to equations (10)-(12).

By way of example, the uncertainty assessment of F_x is presented in the following tables. In table 6, the individual uncertainty contributions, evaluated at load level #1, i.e. -5233.6 N, are shown. Uncertainty contribution due to the applied reference force or moment is, in general terms, the major uncertainty contribution, except for F_z whose main one is due to reproducibility. Systematic component $\Delta(F_{x,1})$ is rather low compared to the random ones.

Table 6. Uncertainty contribution associated with F_x at load level #1, -5233.6 N.

$u_1(F_{x,1}) / \text{N}$	100.7
$u_2(F_{x,1}) / \text{N}$	23.4
$u_3(F_{x,1}) / \text{N}$	18.8
$u_4(F_{x,1}) / \text{N}$	0.1
$\Delta(F_{x,1}) / \text{N}$	4.7
$U(F_{x,1}) / \text{N}$	214.8

In table 7, the expanded uncertainties associated with F_x for each load level are reported. Expanded uncertainties increase at increasing positive or negative levels. It is worth noting that the lowest load level represents the 2.6 % of the nominal capacity of the MCFMT declared by the manufacturer, thus higher uncertainties are expected. It is possible to perform a linear regression of data (positive-only, negative-only, or both) with a second-order polynomial function and get the expanded uncertainty as a function of the applied load. For example, second-order polynomial equation terms of the eight data for side force F_x are reported in equation (17) and figure 7. Absolute and relative expanded uncertainties of all force and moment components are shown in tables (8)-(12). Relative expanded uncertainties are referred

to the nominal MCFMT capacity. Absolute uncertainties increase at increasing loads, while relative ones are almost constant within the considered range.

Table 7. Expanded uncertainties associated with F_x at each j^{th} load level.

$F_{x,j} / \text{N}$	$U(F_{x,j}) / \text{N}$	$U(F_{x,j})/F_{x,c}$
-5233.6	214.8	1.07×10^{-2}
-4186.9	180.7	9.04×10^{-3}
-2616.8	118.6	5.93×10^{-3}
-523.4	50.5	2.52×10^{-3}
523.4	55.8	2.79×10^{-3}
2616.8	115.5	5.78×10^{-3}
4186.9	174.4	8.72×10^{-3}
5233.6	213.9	1.07×10^{-2}

$$U(F_x) = 6 \cdot 10^{-6} \cdot F_x^2 - 0.0004 \cdot F_x + 64.839 \quad (17)$$

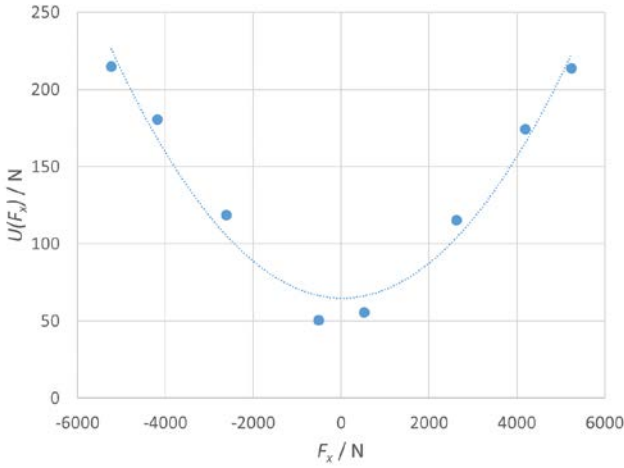


Figure 7. Expanded uncertainties associated with F_x as a function of the applied load.

Table 8. Expanded uncertainties associated with F_y at each j^{th} load level.

$F_{y,j} / \text{N}$	$U(F_{y,j}) / \text{N}$	$U(F_{y,j})/F_{y,c}$
-5233.6	237.6	1.19×10^{-2}
-4186.9	195.7	9.79×10^{-3}
-2616.8	136.4	6.82×10^{-3}
-523.4	95.5	4.78×10^{-3}
523.4	95.5	4.78×10^{-3}
2616.8	137.3	6.87×10^{-3}
4186.9	198.8	9.94×10^{-3}
5233.6	241.1	1.21×10^{-2}

Table 9. Expanded uncertainties associated with F_z at each j^{th} load level.

$F_{z,j} / \text{N}$	$U(F_{z,j}) / \text{N}$	$U(F_{z,j})/F_{z,c}$
9986	224.2	2.24×10^{-3}
49931	305.6	3.06×10^{-3}
79890	327.8	3.28×10^{-3}
99863	299.8	3.00×10^{-3}

Table 10. Expanded uncertainties associated with M_x at each j^{th} load level.

$M_{x,j} / \text{N}\cdot\text{m}$	$U(M_{x,j}) / \text{N}\cdot\text{m}$	$U(M_{x,j})/M_{x,c}$
-1600.0	162.8	8.14×10^{-2}
-1280.0	129.8	6.49×10^{-2}
-800.0	81.7	4.08×10^{-2}
-160.0	40.8	2.04×10^{-2}
160.0	43.7	2.18×10^{-2}
800.0	89.1	4.45×10^{-2}
1280.0	130.5	6.53×10^{-2}
1600.0	157.0	7.85×10^{-2}

Table 11. Expanded uncertainties associated with M_x at each j^{th} load level.

$M_{y,j} / \text{N}\cdot\text{m}$	$U(M_{y,j}) / \text{N}\cdot\text{m}$	$U(M_{y,j})/M_{y,c}$
-1600	222.1	1.11×10^{-1}
-1280	175.9	8.79×10^{-2}
-800	107.3	5.37×10^{-2}
-160	27.0	1.35×10^{-2}
160	27.3	1.37×10^{-2}
800	70.3	3.51×10^{-2}
1280	118.0	5.90×10^{-2}
1600	146.7	7.33×10^{-2}

Table 12. Expanded uncertainties associated with M_x at each j^{th} load level.

$M_{z,j} / \text{N}\cdot\text{m}$	$U(M_{z,j}) / \text{N}\cdot\text{m}$	$U(M_{z,j})/M_{z,c}$
-83.7	9.4	6.29×10^{-3}
-67.0	8.0	5.33×10^{-3}
-41.9	5.9	3.96×10^{-3}
-8.4	3.6	2.42×10^{-3}
8.4	4.5	2.98×10^{-3}
41.9	9.7	6.46×10^{-3}
67.0	12.7	8.48×10^{-3}
83.7	18.4	1.22×10^{-2}

4.4 Comparison between the two methods for uncertainty assessment

It is intuitive that the two methods of uncertainty propagation developed so far, if applied to the same data set, should provide consistent results and shall be verified. For the end-user who has the uncertainties expressed in matrix form, associated with the exploitation matrix, i.e. $U(A)$, the evaluation of the uncertainties associated with the measured forces and moments is relatively simple. Once converted the d_i outputs into forces or moments F_l using equation (2), the uncertainty associated with forces or moments is found by propagating the uncertainties of the exploitation matrix terms $A_{i,l}$ found in Section 4.2, according to equation (18).

$$U(F_l) = 2 \sqrt{\sum_{i=1}^6 u^2(A_{i,l}) d_i^2} \quad (18)$$

On the other hand, end-users who get the expanded uncertainty equations, as seen in Section 4.3, converts the d_i outputs into forces or moments F_i using equation (2), then use the relevant uncertainty equations, e.g. equation (17), to get the associated expanded uncertainty.

Two numerical examples are proposed in order to check the differences between the two methods. The first represents the application of a pure bending moment M_x , the second is the application of all components to their maximum calibration capacity. Values are represented in tables 13 and 14.

Table 13. Expanded uncertainties associated with the application of a pure bending moment M_x evaluated with the two uncertainty methods.

i	$d_i /$ mV/V	$F_i /$ N or N·m	$U(F_i) /$ N or N·m (matrix form)	$U(F_i) /$ N or N·m (ISO 376)
1	0.00000	-16.0	33.8	64.8
2	0.00000	-23.7	34.1	98.1
3	0.00000	253.1	145.8	189.3
4	1.43000	1574.6	27.5	161.8
5	0.00000	-14.4	25.6	38.4
6	0.00000	-2.4	2.2	4.5

Table 14. Expanded uncertainties associated with the application of all components evaluated with the two uncertainty methods.

i	$d_i /$ mV/V	$F_i /$ N or N·m	$U(F_i) /$ N or N·m (Matrix form)	$U(F_i) /$ N or N·m (ISO 376)
1	0.30000	4517.5	80.2	182.0
2	0.30000	4640.0	93.8	214.1
3	1.25000	100561.8	315.0	301.8
4	1.31000	1583.4	76.0	163.1
5	1.31000	1327.2	95.7	114.3
6	0.07000	75.5	6.0	15.7

Both methods show increasing uncertainties at increasing loads, in accordance with the relevant equations. The uncertainty assessment method in analogy to ISO 376 provides higher uncertainties than the matrix method. This is due to the fact that in matrix form the reproducibility, evaluated only in the second method, cannot be univocally determined for different forces and moments combination, thus a lower uncertainty is expected since only repeatability is assessed. However, although method 2, in analogy to ISO 376, provides higher uncertainties, it seems more feasible and more practical for end-users and subsequent applications.

Conclusions and future works

In this work, a relatively inexpensive and accessible calibration system, together with a suitable calibration procedure for MCFMTs, based on the use of FSMs equipped with tilted plates is described. The vertical force acting on the

MCFMT under calibration is decoupled among the three force components and bending and torsion moments are applied by misaligning the transducer placed between the tilted plates. The advantage of the method is that it is not necessary to devise and develop ad-hoc calibration systems. On the other hand, the main limit is the inability to independently apply forces and moments, which depend on the input variables of the system, as shown in equation (1), that are, the applied vertical force, the angles of tilt and rotation and the misalignments.

This method is applied at INRiM by equipping force standard machines with tilted plates with angles up to 3°. This value is cautiously chosen in order to guarantee the stability of the whole structure during load, which, in turn, depends on the steel-to-steel friction between the tilted plates and transducer surfaces. To increase this value, and consequently to increase the maximum applied side forces and torque which linearly depend on the tilt angle value, the friction between the tilted plate/transducer contact surfaces shall be increased. Uncertainty assessment associated with the applied reference force and moment components is performed. Relative expanded uncertainties associated with side forces and moments are in the order of around 5 % at maximum capacity, while that associated with the vertical force is given by the FSM's CMC, as shown in Section 2.2. By analysing the individual uncertainty contributions, it is found that the major uncertainty contribution in the generation of side forces is due to the rotation and tilt angles, while the misalignment is the major contribution for bending and torsion moments. Decreasing them by an order of magnitude would lower the relative expanded uncertainties down to around 0.5 %. This could be reached by improving the alignment processes, in terms of rotation angle and misalignments, and by increasing the tilt angle.

A calibration procedure for MCFMTs is also proposed and applied to a six-components transducer with a vertical force capacity of 100 kN. Each MCFMT output is nominally related to a single component. An experimental plan with 520 measurement conditions, based on the different input values combinations, is tested in order to get low correlation values between the applied components to reach a low uncertainty level, according to Fisher's theory. Calibration results, in terms of main and cross-talk sensitivities, are shown and obtained from matrix calculations. Two different uncertainty assessment methods, according to GUM, are also described. The first in matrix form, the second in analogy to ISO 376 for uniaxial force transducers.

It is shown that the 6×6 exploitation matrix is characterized by higher values along the diagonal terms, as expected since each output is nominally sensitive to a single component. However, cross-talk terms, due to the interaction of each output to the other components, are not negligible. Calibration uncertainty is evaluated by considering contributions due to

repeatability, reproducibility, return to zero, resolution and reference applied force and moment components. In general terms, it is found that the major uncertainty contributions are due to the applied reference forces and moments. By comparing the two uncertainty assessment methods, it is found the method in analogy to ISO 376 seems simpler and more usable, although it may lead to higher uncertainties.

In the future, the possibility to increase the tilt angle will be evaluated by increasing the friction between the tilted plates and the MCFMT. Preliminary tests on the stability of the whole structure will be performed with numerical simulations and applied to a deadweight machine with lower capacity. Furthermore, an optimized experimental plan will be investigated to further decrease the number of measurements and at the same time to get low correlation values between the applied reference forces and moments. In the end, an improved alignment method with the aid of machines and automatic processes will be investigated and developed in order to decrease the uncertainties associated with the misalignment and rotation angle of the reference applied force and moment components. The method presented in this work is easily implementable by National Metrology Institutes or calibration laboratories and can be adopted to improve the current standard.

Acknowledgments

This work was supported by the EURAMET and the European Union in the framework of EMPIR project ComTraForce [18SIB08, 2019].

References

- [1] Long J, Liang Q, Sun W, Wang Y and Zhang D 2021 Ultrathin Three-Axis FBG Wrist Force Sensor for Collaborative Robots *IEEE Transactions on Instrumentation and Measurement* **70** 1–15
- [2] Grosu V, Grosu S, Vanderborcht B, Lefebvre D and Rodriguez-Guerrero C 2017 Multi-Axis Force Sensor for Human–Robot Interaction Sensing in a Rehabilitation Robotic Device *Sensors* **17** 1294
- [3] Ahmad A R, Wynn T and Lin C Y 2021 A Comprehensive Design of Six-Axis Force/Moment Sensor *Sensors* **21** 4498
- [4] Ewald B 2000 Multi-component force balances for conventional and cryogenic windtunnels *Meas. Sci. Technol.* **11** R81–94
- [5] Tavakolpour-Saleh R, Setoodeh A R and Gholamzadeh M 2016 A novel multi-component strain-gauge external balance for wind tunnel tests: Simulation and experiment *Sensors and Actuators A: Physical* **247** 172–186.
- [6] Liang Q, Zhang D, Wu W, Zou K 2016 Methods and Research for Multi-Component Cutting Force Sensing Devices and Approaches in Machining *Sensors* **16** 1926
- [7] Genta G, Prato A, Mazzoleni F, Germak A and Galetto M 2018 Accurate force and moment measurement in spring testing machines by an integrated hexapod-shaped multicomponent force transducer *Meas. Sci. Technol.* **29** 095902
- [8] Nitsche J, Baumgarten S, Petz M, Röske D, Kumme R and Tutsch R 2017 Measurement uncertainty evaluation of a hexapod-structured calibration device for multi-component force and moment sensors *Metrologia* **54**(2) 171
- [9] Röske D 2003 Metrological characterization of a hexapod for a multi-component calibration device *XVII IMEKO World Congress*
- [10] Baumgarten S, Röske D and Kumme R 2017 Multi-component measuring device - completion, measurement uncertainty budget and signal cross-talk for combined load conditions *ACTA IMEKO* **6**(4)
- [11] Kim G-S 2000 The development of a six-component force/moment sensor testing machine and evaluation of its uncertainty *Meas. Sci. Technol.* **11** 1377–82
- [12] Kim G-S and Yoon J 2007 Development of calibration system for multi-axis force/moment sensor and its uncertainty evaluation *J. Korean Soc. Prec. Eng.* **24** 91–8
- [13] Ferrero C, Zhong L Q, Marinari C and Martino E 1993 New automatic multicomponent calibration system with crossedflexure levers *The 3rd Int. Symp. on Measurement and Control in Robotics* Cm.I-31–Cm.I-39
- [14] Bray A, Barbato G and Levi R 1990 Theory and practice of force measurement *Academic Press, London, UK*
- [15] Barbato G, Bray A, Desogus S, Franceschini F and Germak A 1992 Field calibration method for multicomponent robotic force/moment transducers *II International Symposium on Measurement and Control in Robotics*
- [16] BIPM 2017 Consultative Committee for Mass and Related Quantities (CCM) Strategy plan 2017 to 2027. <https://www.bipm.org/documents/20126/2071009/CCM+Strategic+Plan.pdf/1bd953eb-c2b5-7cd2-cee7-48de2747e52a> (Last access 12 November 2021).
- [17] Palumbo S, Prato A, Mazzoleni F and Germak A 2018 Multicomponent force transducer calibration procedure using tilted plates *XXII World Congress*
- [18] JCGM 100:2008 Evaluation of Measurement Data — Guide to the Expression of Uncertainty in Measurement (GUM), Joint Committee for Guides in Metrology, Sèvres, France.
- [19] ISO 376:2011 — Metallic materials — Calibration of force-proving instruments used for the verification of uniaxial testing machines
- [20] Baumgarten S, Kahmann H and Röske D 2001 Metrological characterization of a 2 kN·m torque standard machine for superposition with axial forces up to 1 MN *Metrologia* **53** 1165–76
- [21] Fisher R 1926 The Arrangement of Field Experiments *Journal of the Ministry of Agriculture of Great Britain* **33** 503–513
- [22] Prato A, Borgiattino D, Mazzoleni F, Facello A and Germak A 2021 Theoretical insights on the influence of the experimental plan in the calibration of multicomponent force and moment transducers *Measurement: Sensors* **18** 100209
- [23] Prato A, Mazzoleni F and Schiavi A 2020 Traceability of digital 3-axis MEMS accelerometer: simultaneous determination of main and transverse sensitivities in the frequency domain *Metrologia* **57**(3) 035013